

Supplementary Tables and Figures for “Genome-Wide Prediction of cis-Regulatory Regions Using Supervised Deep Learning Methods”

Yifeng Li^{*1,2}, Wenqiang Shi^{†1}, and Wyeth W. Wasserman^{‡1}

¹Centre for Molecular Medicine and Therapeutics, BC Children’s Hospital Research Institute, Department of Medical Genetics, University of British Columbia

²Digital Technologies Research Centre, National Research Council Canada

Table S1: Numbers of labelled regions in our data.

Cell	A-E	I-E	A-P	I-P	A-X	I-X	UK	Total
A549	387	40,387	10,907	128,998	8,998	14,712	81,217	285,606
GM12878	2,878	28,156	10,816	73,891	8,226	19,078	80,004	223,049
HelaS3	1847	32,179	10,759	79,009	9,123	22,071	81,502	236,485
HepG2	1465	34,556	11,467	96,184	9,931	19,071	79,417	252,091
HUVEC	1226	35,143	11,254	101,861	9,739	18,249	80,333	257,805
K562	894	34,392	10,076	82,829	9,033	20,261	78,081	235,566
MCF7	249	36,873	10,733	81,510	10,829	13,653	82,663	236,510

Table S2: Number of features used for each cell type and number of common features between any two cell types in our labelled data.

Cell	A549	GM12878	HelaS3	HepG2	HMEC	HUVEC	K562	MCF7
A549	45	38	26	38	15	19	38	25
GM12878	-	101	50	54	16	21	69	26
HelaS3	-	-	74	43	16	22	56	23
HepG2	-	-	-	72	16	21	57	28
HMEC	-	-	-	-	16	16	16	9
HUVEC	-	-	-	-	-	24	24	13
K562	-	-	-	-	-	-	135	29
MCF7	-	-	-	-	-	-	-	38

*E-mail address: yifeng@cmmt.ubc.ca, and yifeng.li@nrc-cnrc.gc.ca.

†E-mail address: shi@cmmt.ubc.ca.

‡Corresponding author, E-mail address: wyeth@cmmt.ubc.ca.

Table S3: Confusion matrices of classifying CRE-seq and MPRA validated regions using DECRES.

Original Class\DECRES Class	A-E	A-P	BG	Total
CRE-seq Positive Combined Predicted Enhancer in K562	254	0	132	386
CRE-seq Negative Combined Predicted Enhancer in K562	433	1	378	812
Combined Predicted Repressed Region in K562	0	0	298	298
Total	687	1	808	1496
MPRA Positive Enhancer in K562	120	0	2	122
MPRA Negative Enhancer in K562	179	0	15	194
Total	299	0	17	316
MPRA Positive Enhancer in HepG2	182	1	3	186
MPRA Negative Enhancer in HepG2	217	5	45	267
Total	399	6	48	453

Table S4: Numbers of predicted and cell-specific *cis*-regulatory regions in the whole human genome. Columns 2-3: results of two-class prediction. Columns 4-7: results of three class prediction.

Cell	A-E+A-P	Specific	A-E	Specific	A-P	Specific
GM12878	90,192	27,904	70,905	27,185	19,287	6,090
HelaS3	100,102	22,268	92,509	22,866	7,593	979
HepG2	114,873	35,986	105,007	41,109	9,866	2,135
HMEC	104,621	28,774	88,803	26,262	15,818	3,043
HUVEC	110,347	16,415	97,069	35,073	13,278	582
K562	133,940	30,835	122,321	56,374	11,619	371

Table S5: Numbers of predicted A-Es and A-Ps on the 102,021 BDT loci. AiA: Active in the FANTOM Enhancer Atlas. IiA: Inactive in the FANTOM Enhancer Atlas. NiA: Not included in the FANTOM Enhancer Atlas. Specific: Predicted cell-specific A-Es.

Cell	A-E	A-P	BG
GM12878	11,910	1,975	88,136
HelaS3	12,743	226	89,052
HepG2	10,761	488	90,772
HMEC	13,356	1,267	87,398
HUVEC	17,192	758	84,071
K562	13,936	288	87,797

Table S6: Overlap between our predicted A-Es and the FANTOM enhancer atlas.

Cell\Element	AiA	IiA	NiA	Specific
GM12878	2,088	5,144	4,678	4,199
HelaS3	1,459	6,435	4,849	1,073
HepG2	1,178	4,888	4,695	1,495
HMEC	1,250	6,644	5,462	1,916
HUVEC	879	8,716	7,597	3,560
K562	750	7,383	5,803	2,965

Table S7: Transcription factors whose binding motifs are enriched in specific cells.

Cell	Transcription Factor	Functionality
GM12878	RUNX1	RUNX1 and other Runt-related factors play crucial roles in haematopoiesis. Translocation of RUNX1 leads to severe acute myeloid leukemia [11].
GM12878	REL/NF- κ B Factors	Play a critical role in immune response to infection [4].
HelaS3	C/EBP-Related Factors	C/EBP-related factors, a subfamily of the basic leucine zipper factors (bZIP), regulating genes involved in immune and inflammatory responses, are expressed in cervix [1].
HelaS3	CREB-Related Factors (Another bZIP Subfamily)	Possibly up-regulate Bcl-2 expression in apoptotic HeLa cells induced by trichosanthin [15].
HelaS3	TEAD1	Plays a role of apoptotic resistance in Hela cells [9].
HelaS3	AP-2 Factors	Can act as tumor suppressor, and malfunction of AP-2 was found in cervical cancer cells [2].
HelaS3	HOX Factors	a subgroup of HOX genes involve in cervical carcinoma [8].
HepG2	HNF1A, HNF1B, FOXA1, FOXA2, HNF4A, and HNF4G	These factors are hepatocyte nuclear factors that regulate liver-specific genes [3, 16].
HepG2	C/EBPs	Have a pivotal role in liver development and function [13].
HMEC	TEAD Family	Members of this family regulate epithelial-mesenchymal transition [17].
HUVEC	GATA Factors	Involve in networks of key determinants of vascular endothelial cell identity [7].
HUVEC	SOX Factors	Regulate vascular cell development and growth (vasculogenesis) [12].
HUVEC	CREB-Related Factors	Involve in several specific pathways in HUVEC cell [14].
K562	GATA-Type, NFYA, and NFYB USF1	The NFY factors cooperate with GATA1 to mediate erythroid-specific transcription, and coassociate with FOS binding to both promoters and enhancers in K562 [5]. The NFY factors are also found cooperate with USF1 and USF2 to active HOXB4 for hematopoiesis [18].
K562	STAT5	Maintains the high-level cell proliferation of K562 [10].

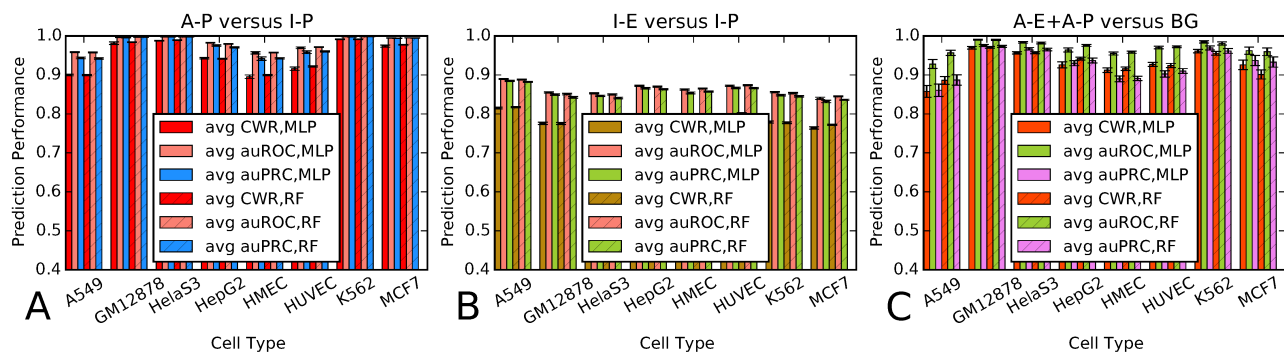


Figure S1: Mean performance and standard deviation of 10-fold cross-validations using the MLP model on our labelled data of eight cell types. A-E: Active Enhancer, A-P: Active Promoter, A-X: Active Exon, I-E: Inactive Enhancer, I-P: Inactive Promoter, I-X: Inactive Exon, UK: Unknown or Uncharacterized, BG: I-E+I-P+A-X+I-X+UK.

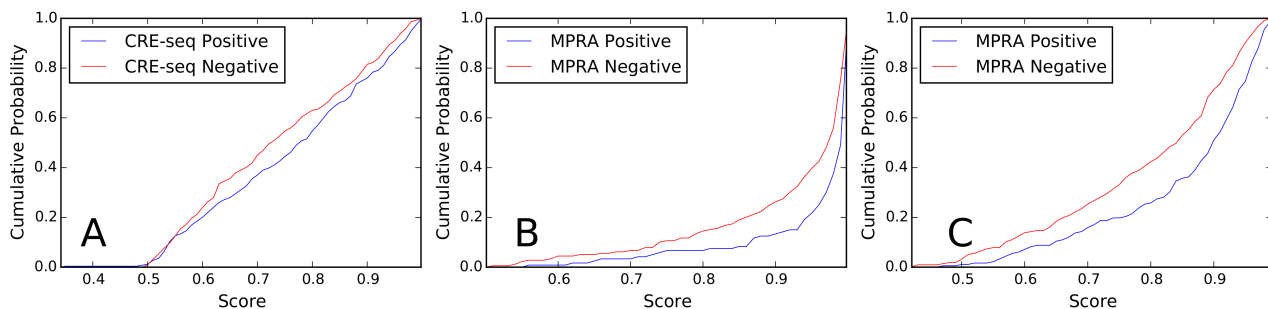


Figure S2: Cumulative DECREASE membership probabilities (scores) of enhancers that were tested as positives and negatives by CRE-seq or MPRA. These enhancers were predicted as A-Es by DECREASE (See Table S3).

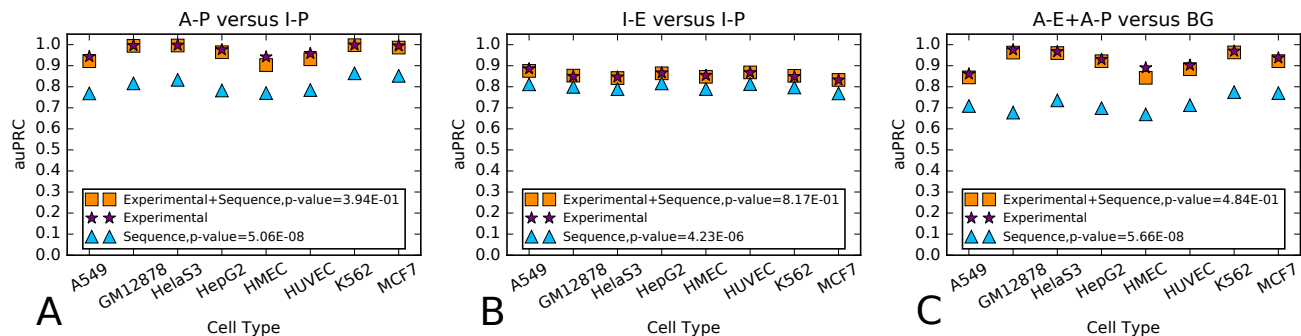


Figure S3: Comparing the mean auPRCs over 100 resampling and retraining on our labelled regions using different feature sets. “Experimental” means our experimentally derived next generation sequencing feature set. “Sequence” means the set of 351 sequence properties used in [6]. “Experimental+Sequence” means the combination of these two sets. The p -values in each legend were obtained using two-tailed Student’s t -test to compare “Experimental”-based results with “Experimental+Sequence”-based and “Sequence”-based results, respectively.

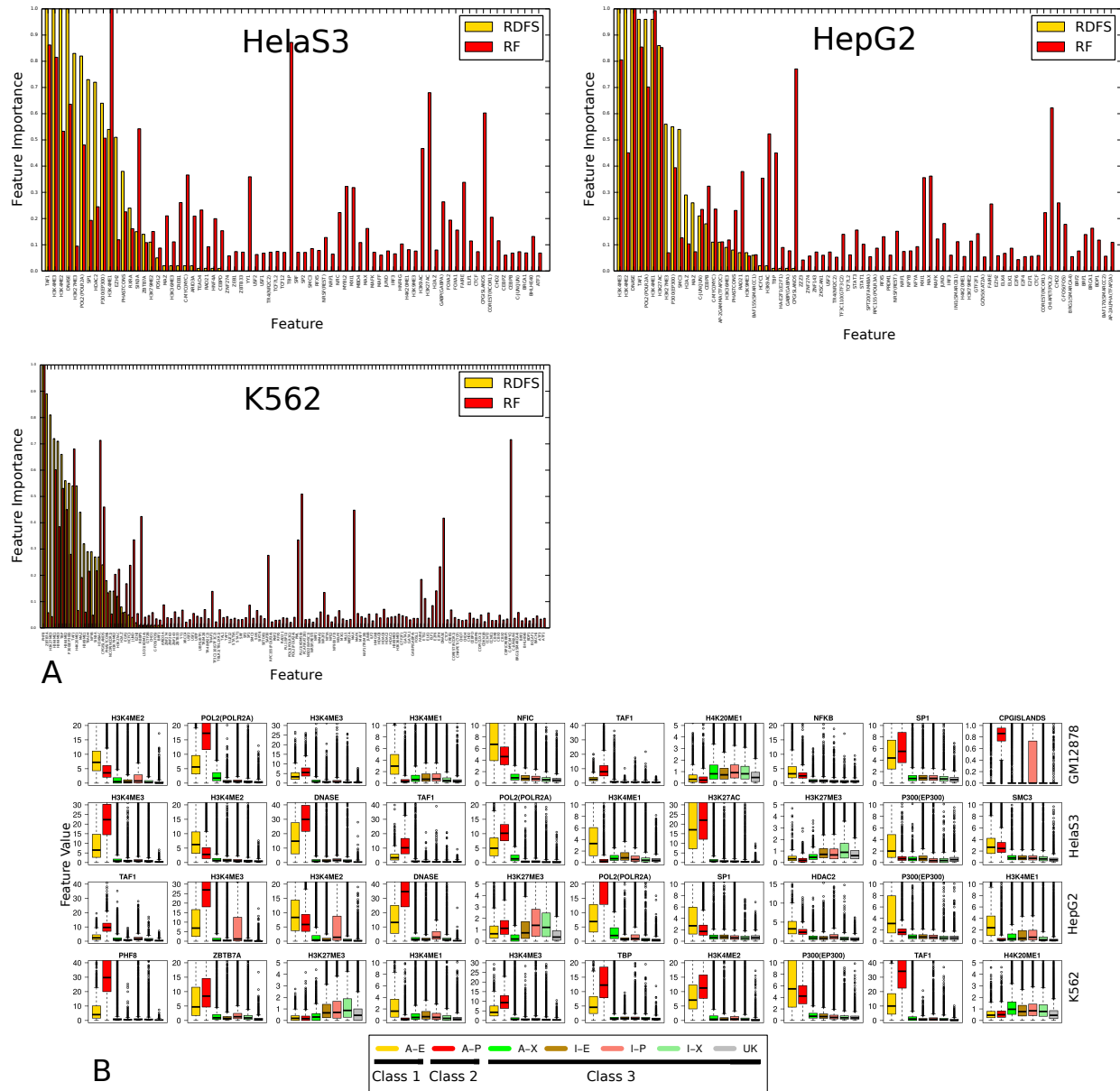


Figure S4: Feature importance and box plots of top features in the 3-class (A-E versus A-P versus BG) scenario. A: Feature importance discovered by randomized DFS (RDFS) and random forest (RF) on HeLaS3, HepG2 and K562 cells. RF's feature importance scores were normalized to [0,1] for better comparison with RDFS. B: For the top 10 features of the 3-class models generated for four well-characterized cell lines, box plots depict the range of observed feature values (log2 scale) for 7 sequence classes.

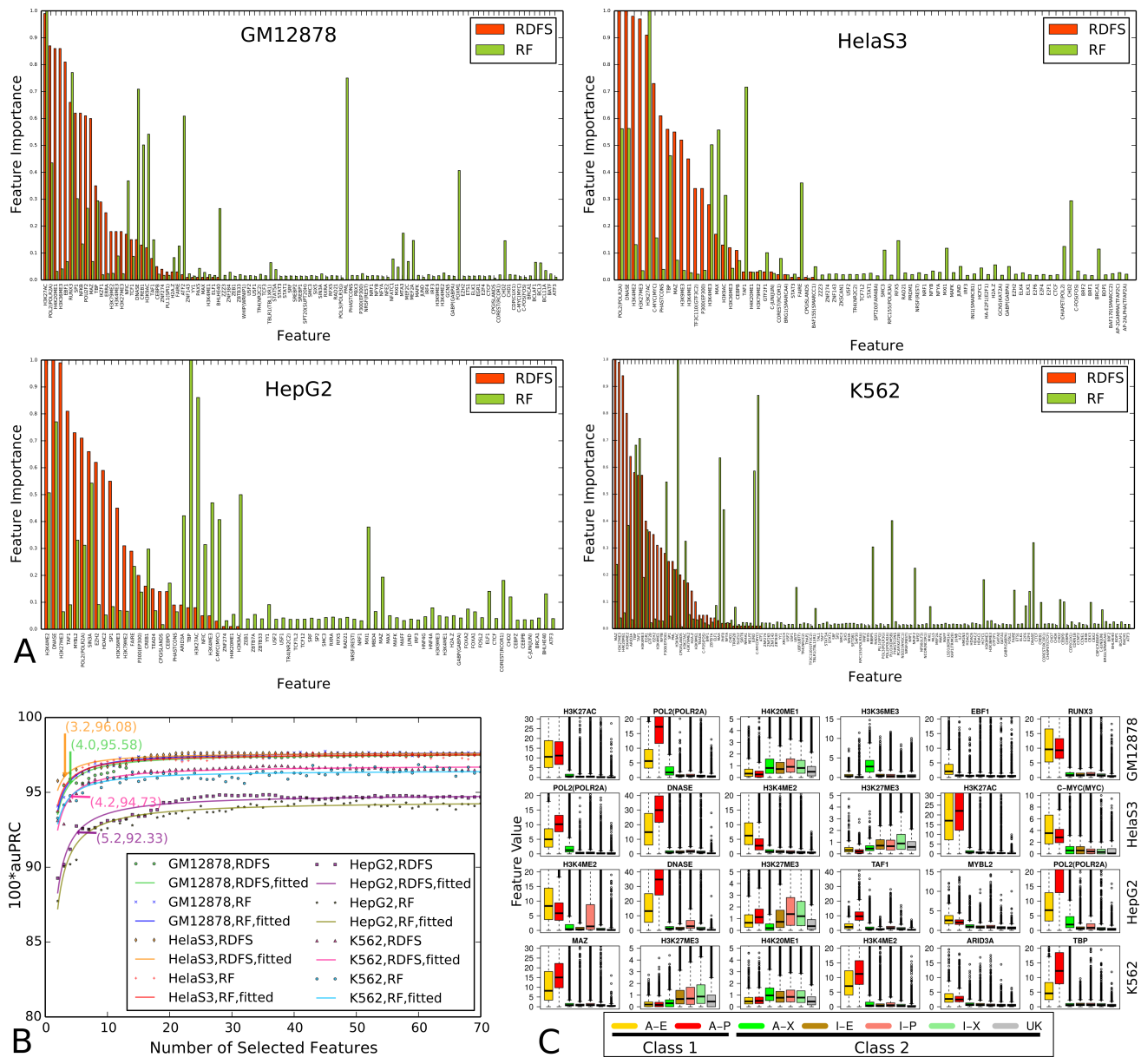


Figure S5: Feature importance, classification performance, and top features in the 2-class (A-E+A-P versus BG) scenario. A: Feature importance discovered by randomized DFS (RDFS) and random forest (RF). The random forest's feature importance scores were normalized to [0,1] for better comparison with randomized DFS. B: auPRC versus the number of features incorporated into the RDFS and RF. The annotated points indicate where a line with slope 0.5 intersects a fitted curve). C: For the top 6 features of the 2-class models generated for four well-characterized cell lines, box plots depict the range of observed feature values (log₂ scale) for 7 sequence classes.

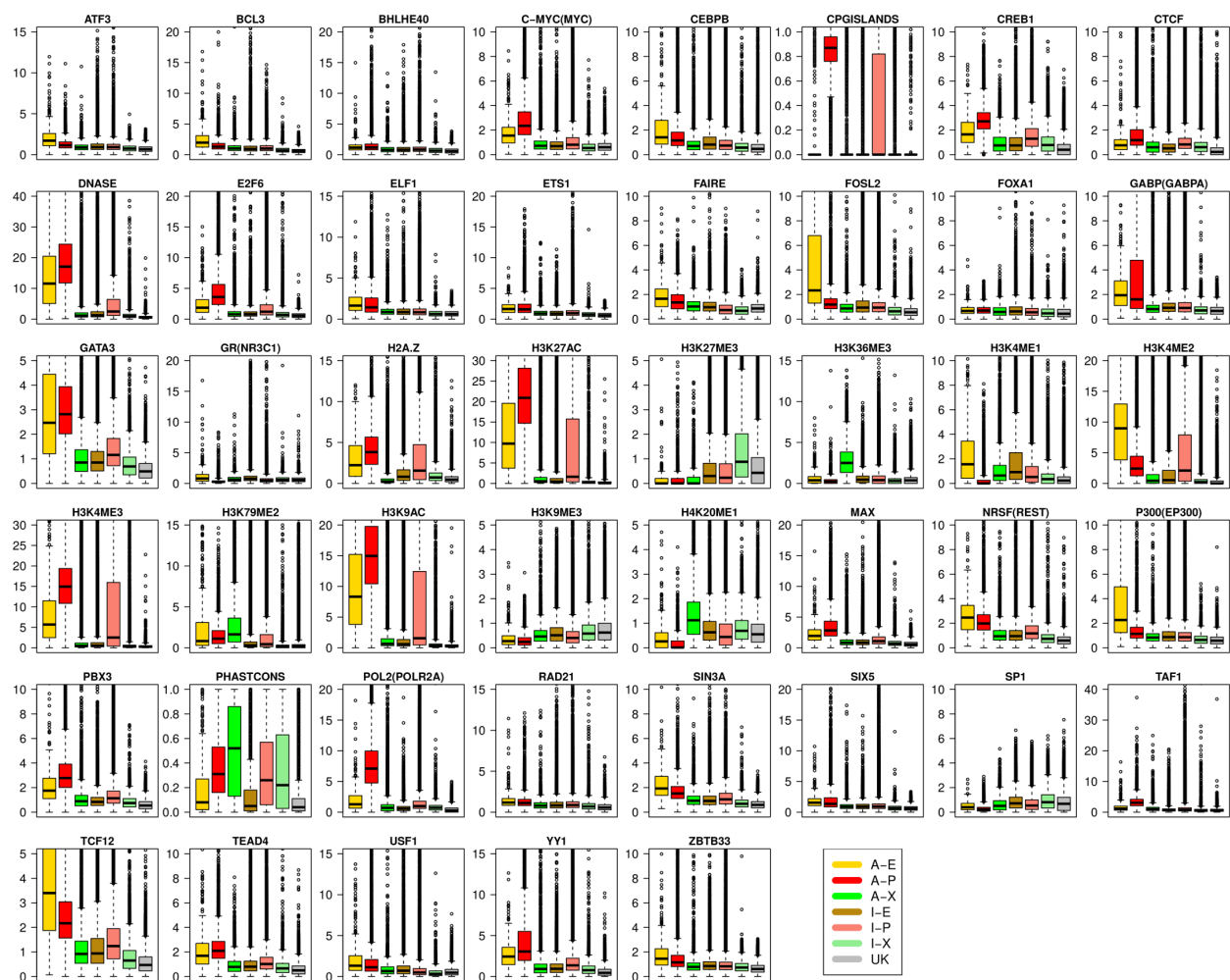


Figure S6: Box plots of all features for A549.

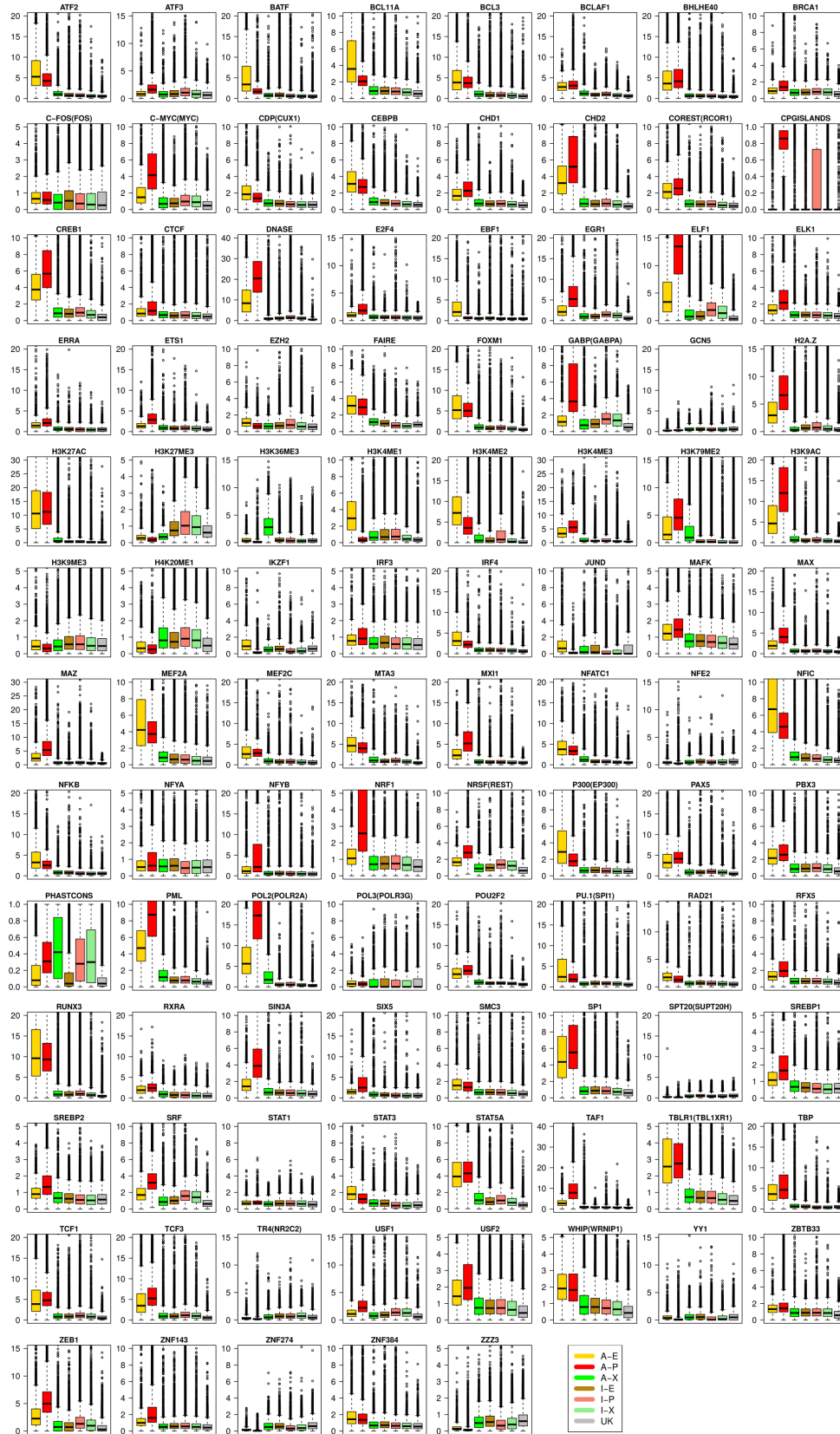


Figure S7: Box plots of all features for GM12878.

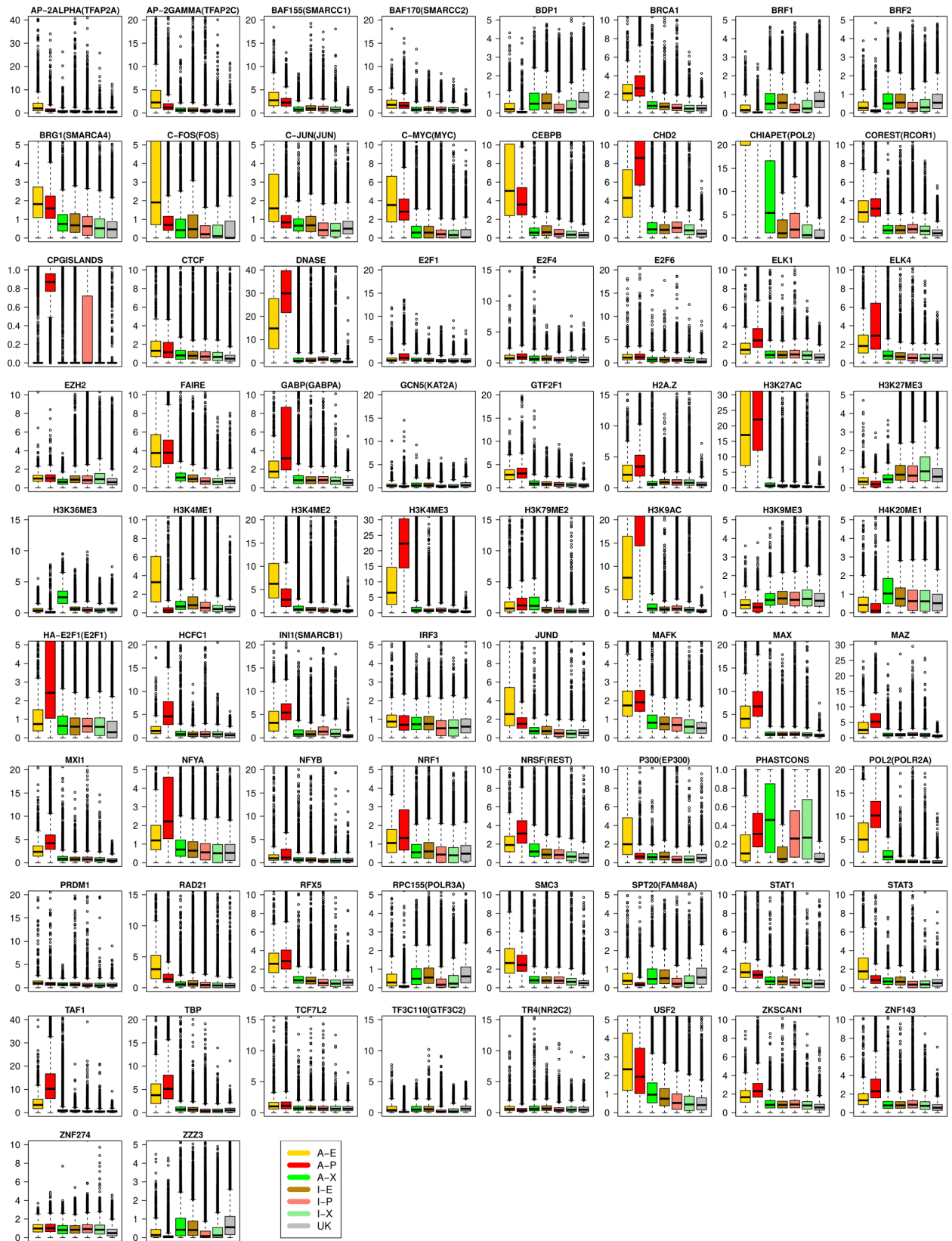


Figure S8: Box plots of all features for Helas3.

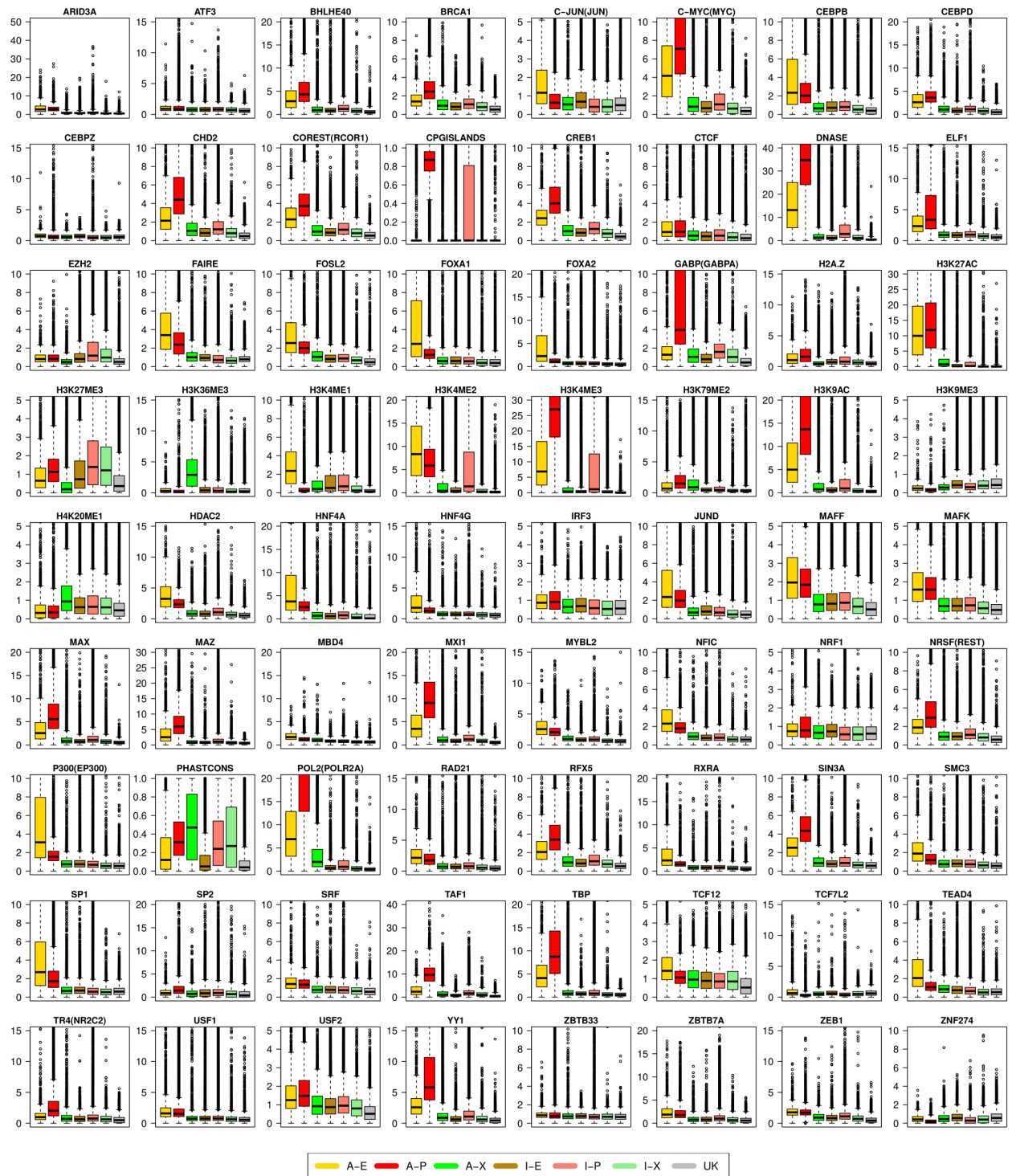


Figure S9: Box plots of all features for HepG2.

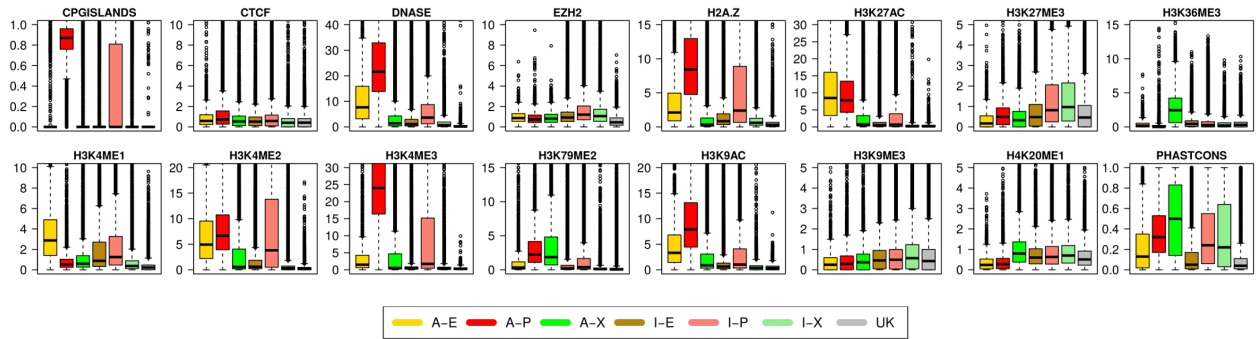


Figure S10: Box plots of all features for HMEC.

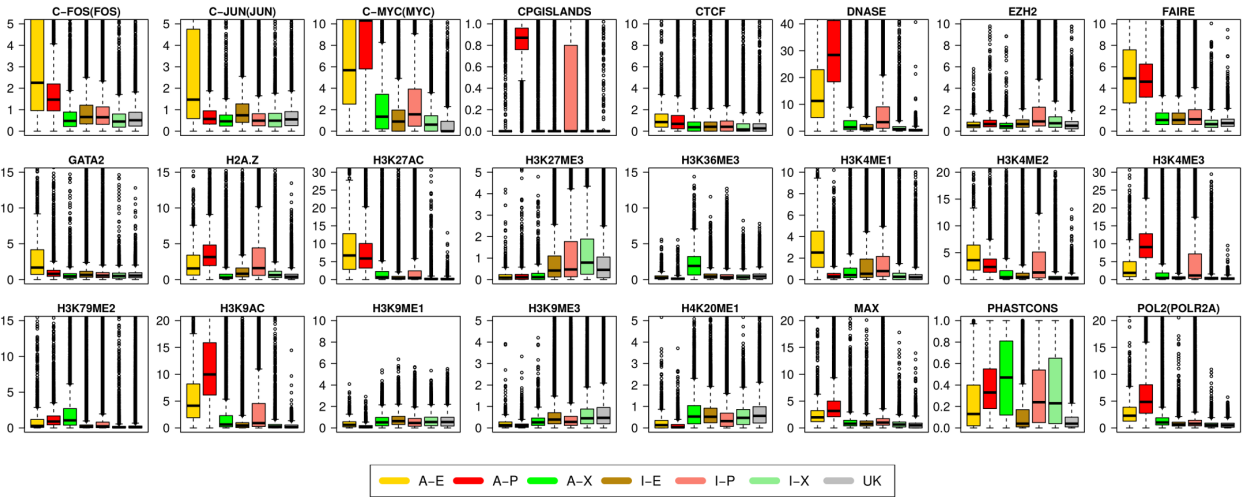


Figure S11: Box plots of all features for HUVEC.

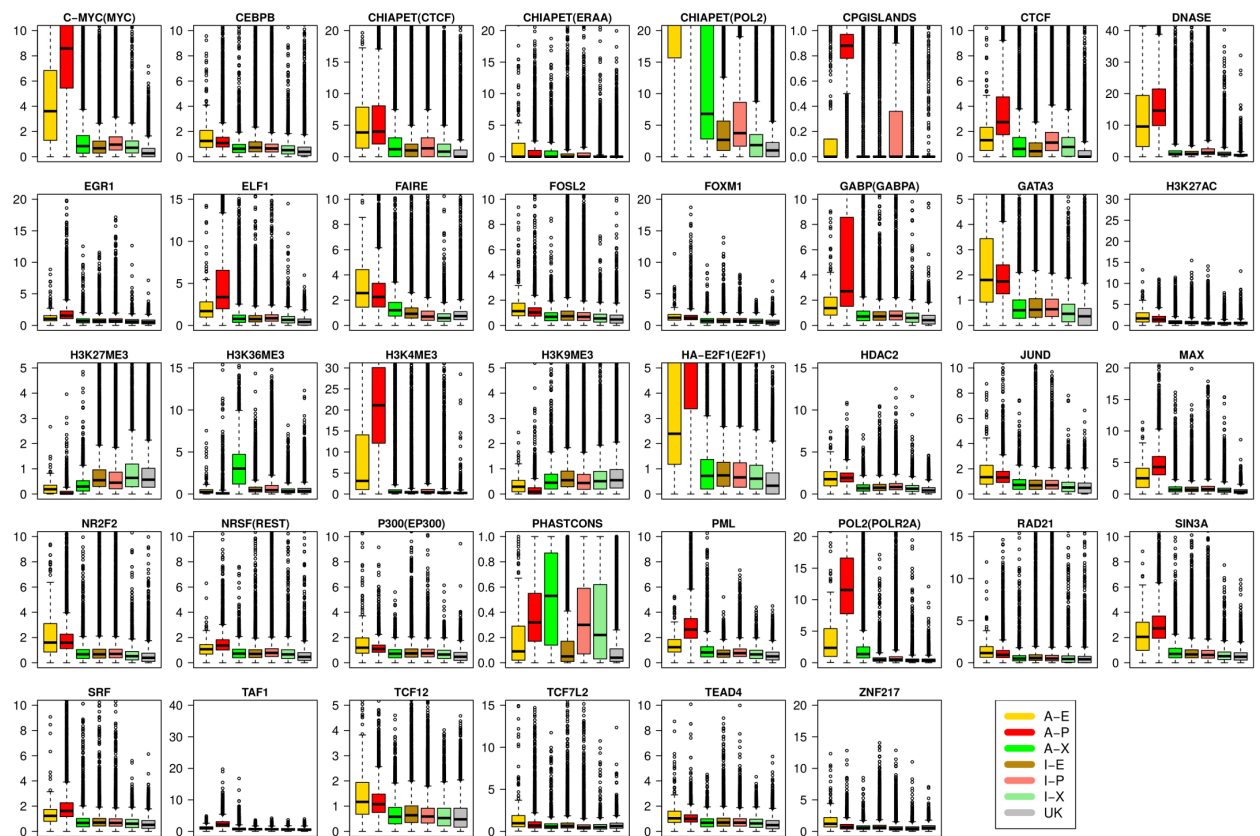


Figure S12: Box plots of all features for MCF7.

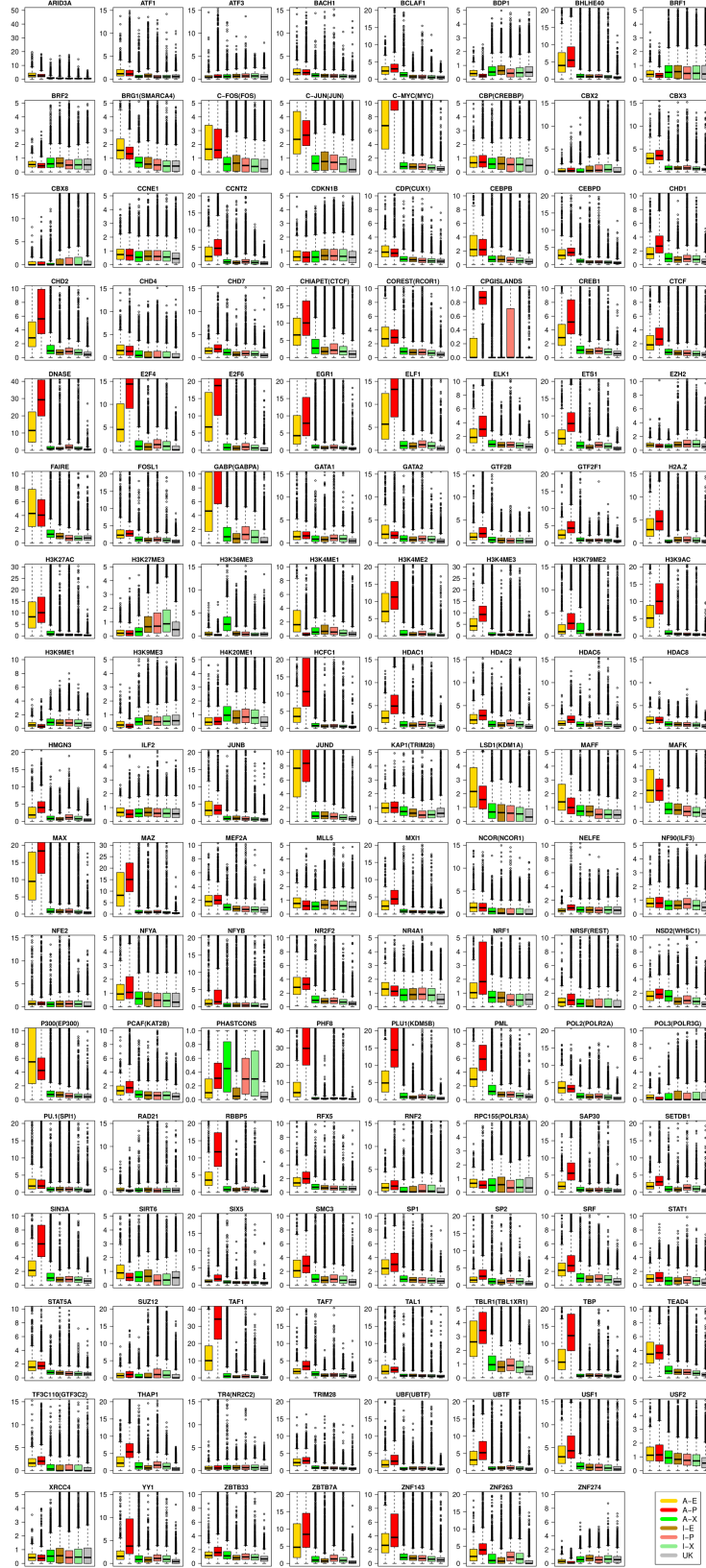


Figure S13: Box plots of all features for K562.

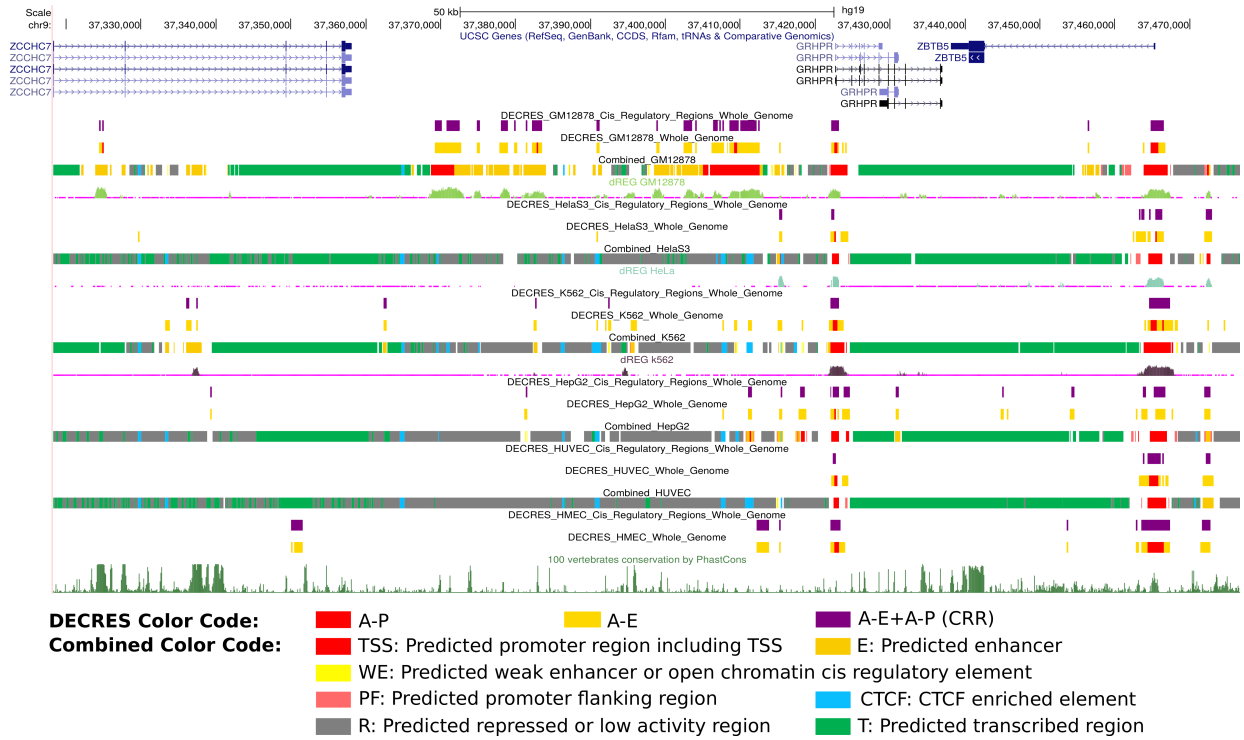


Figure S14: An example of predicted regulatory regions in the UCSC Genome Browser.

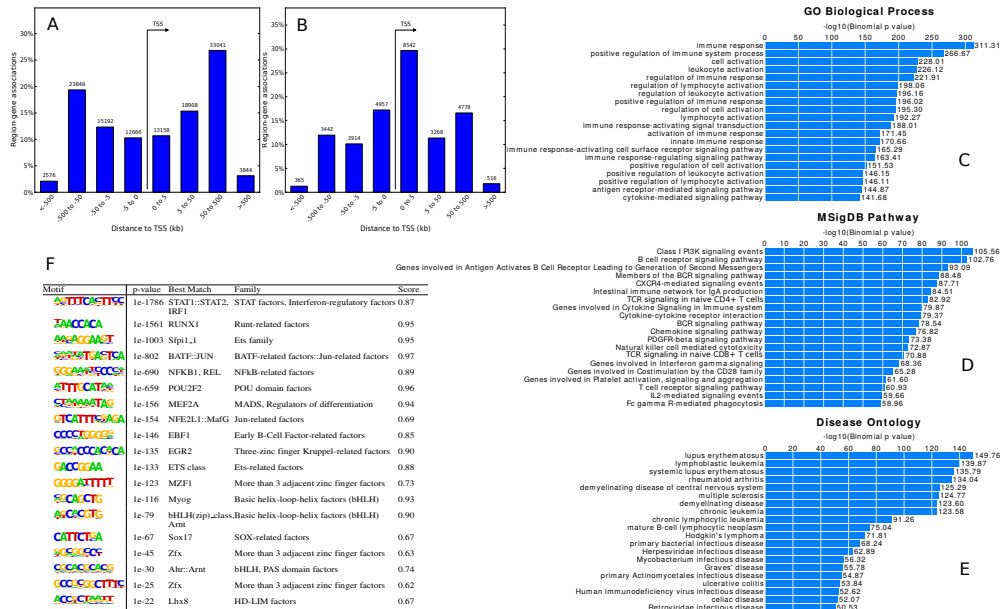


Figure S15: Functional and motif analysis of the DECRES genome-wide predictions on cell line GM12878. A: Distance from the predicted A-Es to gene TSSs. B: Distance from the predicted A-Ps to gene TSSs. C,D,E: Top 20 enriched biological processes, pathways, and diseases, respectively, in the predicted cell-specific CRRs. F: Enriched *de novo* motifs in the predicted cell specific CRRs. Column 4: families of best-matched TFs. Column 5: best match scores.



Figure S16: Functional and motif analysis of the DECRES NiA enhancers on cell line GM12878. A,B,C: Top 20 enriched biological processes, pathways, and diseases, respectively, in the NiA enhancers. D: Enriched *de novo* motifs in the NiA enhancer regions. Column 4: the families of best-matched TFs. Column 5: best match scores.

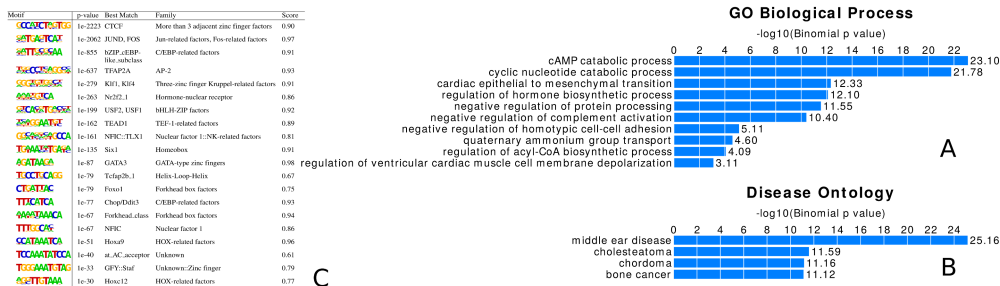


Figure S17: Functional and motif analysis of the DECRES genome-wide predictions on cell line HeLaS3. A,B: Top enriched biological processes and diseases (no pathways enriched for HeLaS3), respectively, in the predicted cell-specific CRRs. C: Enriched *de novo* motifs in the predicted cell specific CRRs. Column 4: families of best-matched TFs. Column 5: best match scores.

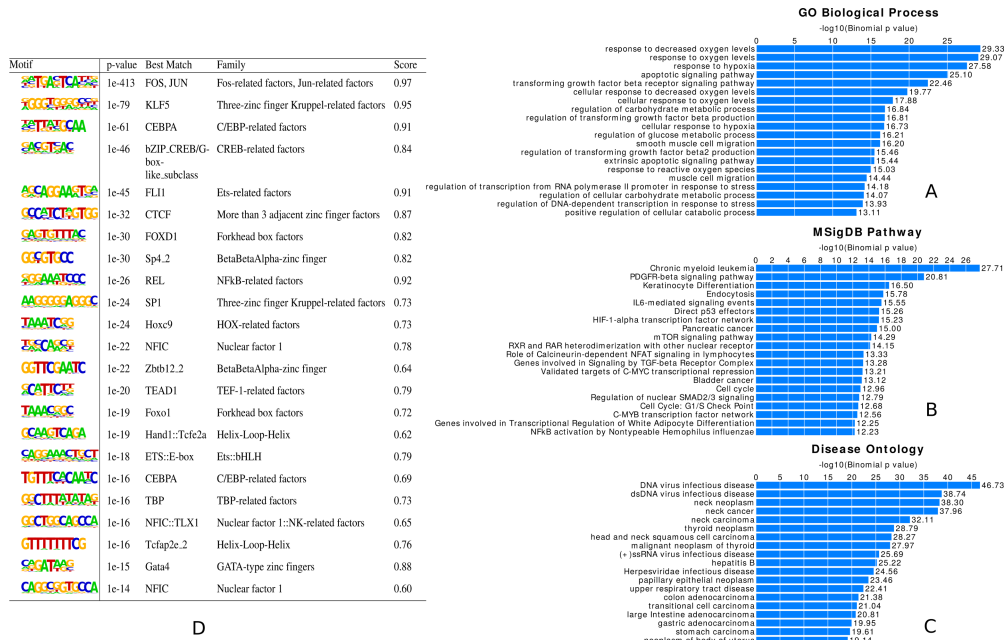


Figure S18: Functional and motif analysis of the DECRES NiA enhancers on cell line HeLaS3. A,B,C: Top 20 enriched biological processes, pathways, and diseases, respectively, in the NiA enhancers. D: Enriched *de novo* motifs in the NiA enhancer regions. Column 4: families of best-matched TFs. Column 5: best match scores.

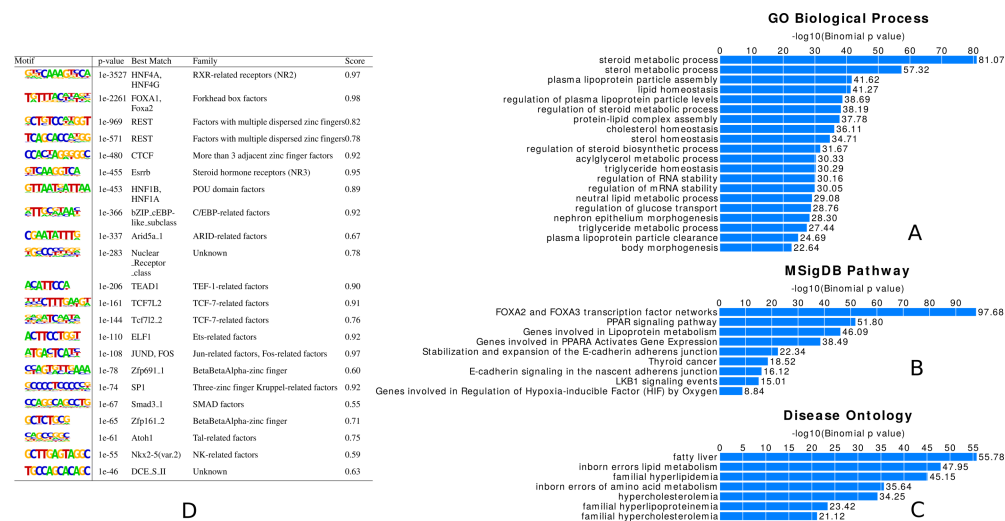


Figure S19: Functional and motif analysis of the DECRES genome-wide predictions on cell line HepG2. A,B,C: Top enriched biological processes, pathways and diseases, respectively, in the predicted cell-specific CRRs. D: Enriched *de novo* motifs in the predicted cell specific CRRs. Column 4: families of best-matched TFs. Column 5: best match scores.



Figure S20: Functional and motif analysis of the DECRES NiA enhancers on cell line HepG2. A,B,C: Top 20 enriched biological processes, pathways, and diseases, respectively, in the NiA enhancers. D: Enriched *de novo* motifs in the NiA enhancer regions. Column 4: families of best-matched TFs. Column 5: best match scores.

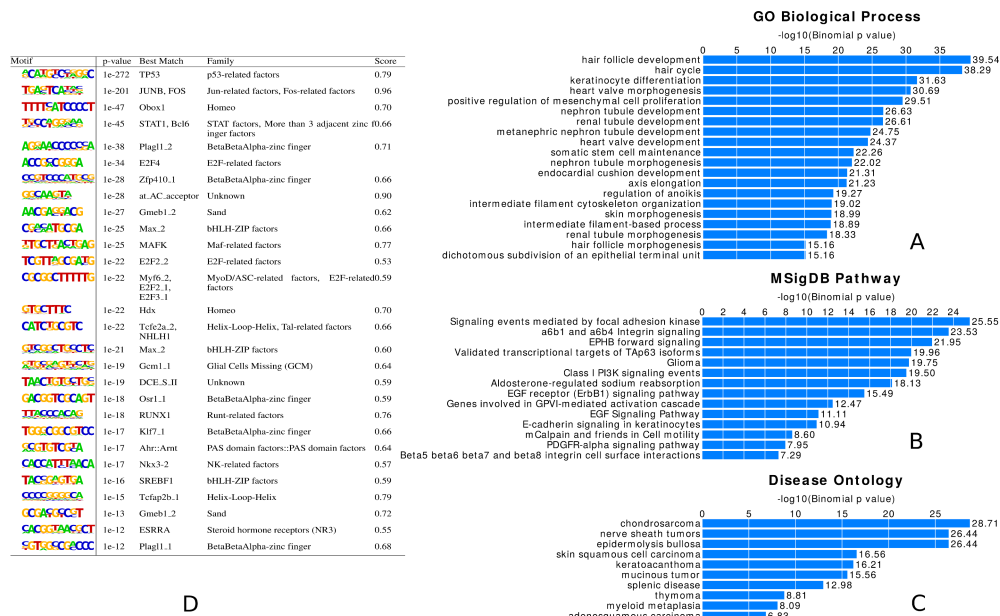


Figure S21: Functional and motif analysis of the DECRES genome-wide predictions on cell line HMEC. A,B,C: Top enriched biological processes, pathways and diseases, respectively, in the predicted cell-specific CRRs. D: Enriched *de novo* motifs in the predicted cell specific CRRs. Column 4: families of best-matched TFs. Column 5: best match scores.

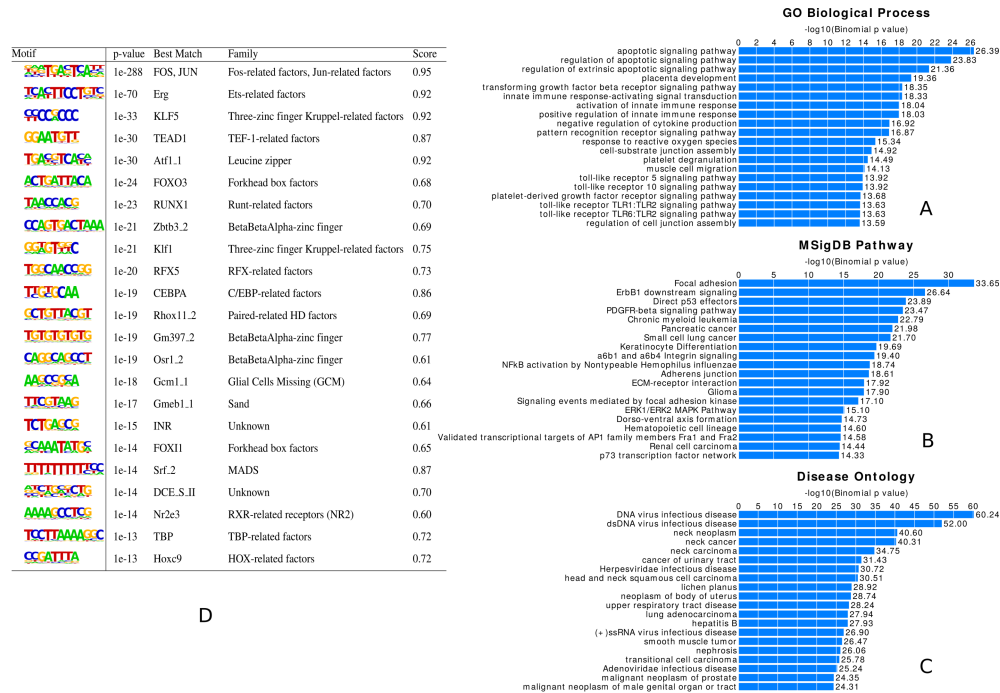


Figure S22: Functional and motif analysis of the DECRES NiA enhancers on cell line HMEC. A,B,C: Top 20 enriched biological processes, pathways, and diseases, respectively, in the NiA enhancers. D: Enriched *de novo* motifs in the NiA enhancer regions. Column 4: families of best-matched TFs. Column 5: best match scores.

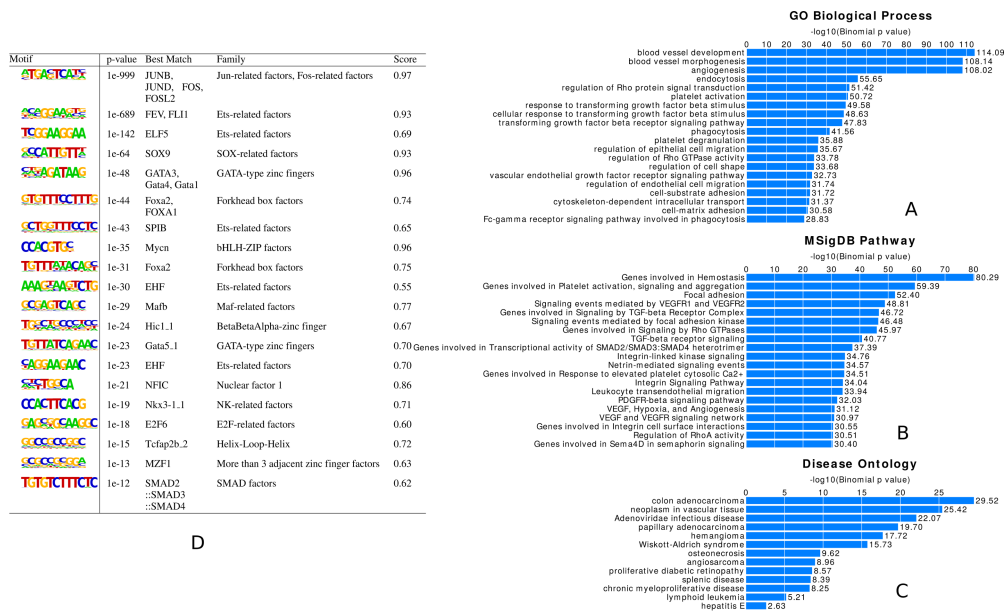


Figure S23: Functional and motif analysis of the DECRES genome-wide predictions on cell line HUVEC. A,B,C: Top enriched biological processes, pathways, and diseases, respectively, in the predicted cell-specific CRRs. D: Enriched *de novo* motifs in the predicted cell specific CRRs. Column 4: families of best-matched TFs. Column 5: best match scores.



Figure S24: Functional and motif analysis of the DECRES NiA enhancers on cell line HUVEC. A,B,C: Top 20 enriched biological processes, pathways, and diseases, respectively, in the NiA enhancers. D: Enriched *de novo* motifs in the NiA enhancer regions. Column 4: families of best-matched TFs. Column 5: best match scores.

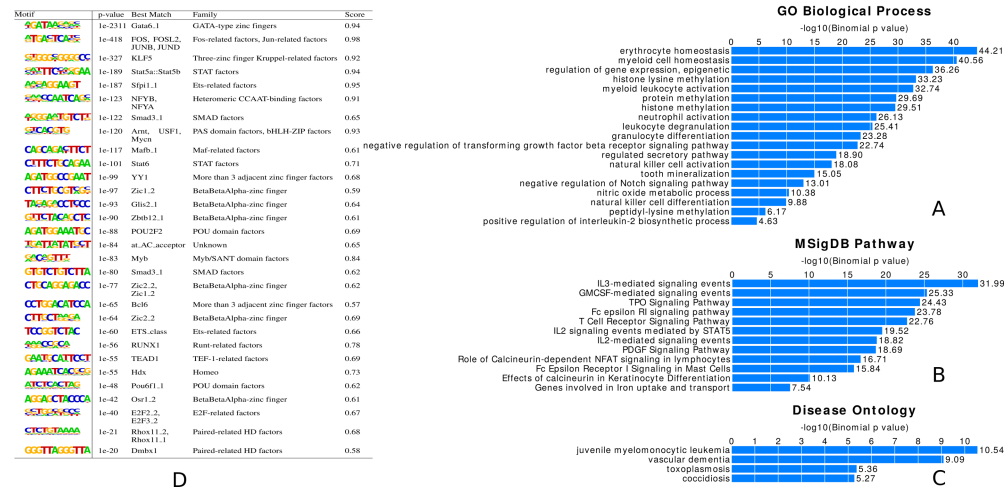


Figure S25: Functional and motif analysis of the DECRES genome-wide predictions on cell line K562. A,B,C: Top enriched biological processes, pathways and diseases, respectively, in the predicted cell-specific CRRs. D: Enriched *de novo* motifs in the predicted cell specific CRRs. Column 4: families of best-matched TFs. Column 5: best match scores.

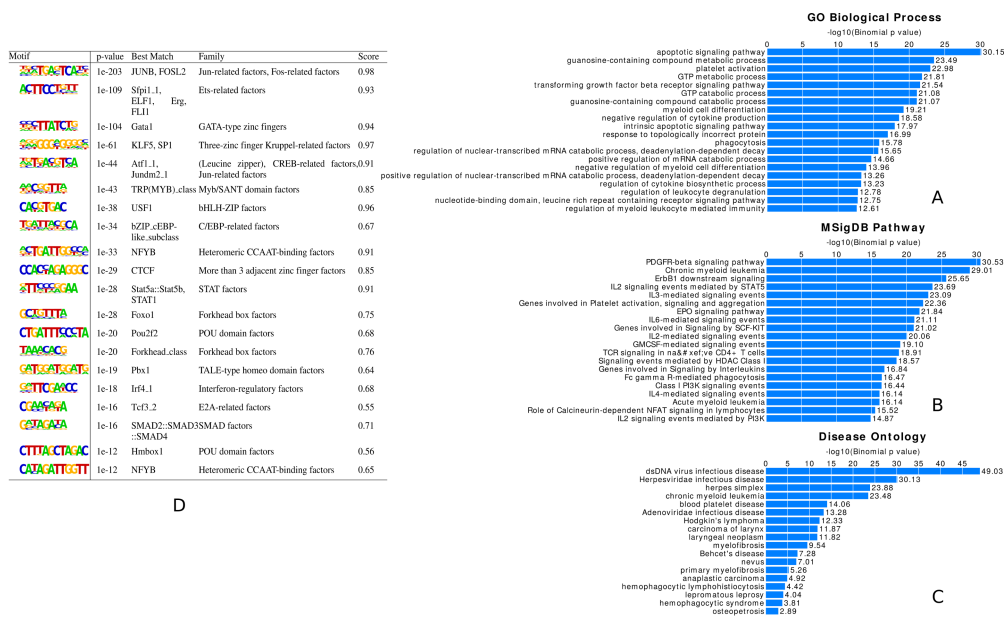


Figure S26: Functional and motif analysis of the DECRES NiA enhancers on cell line K562. A,B,C: Top 20 enriched biological processes, pathways, and diseases, respectively, in the NiA enhancers. D: Enriched *de novo* motifs in the NiA enhancer regions. Column 4: families of best-matched TFs. Column 5: best match scores.

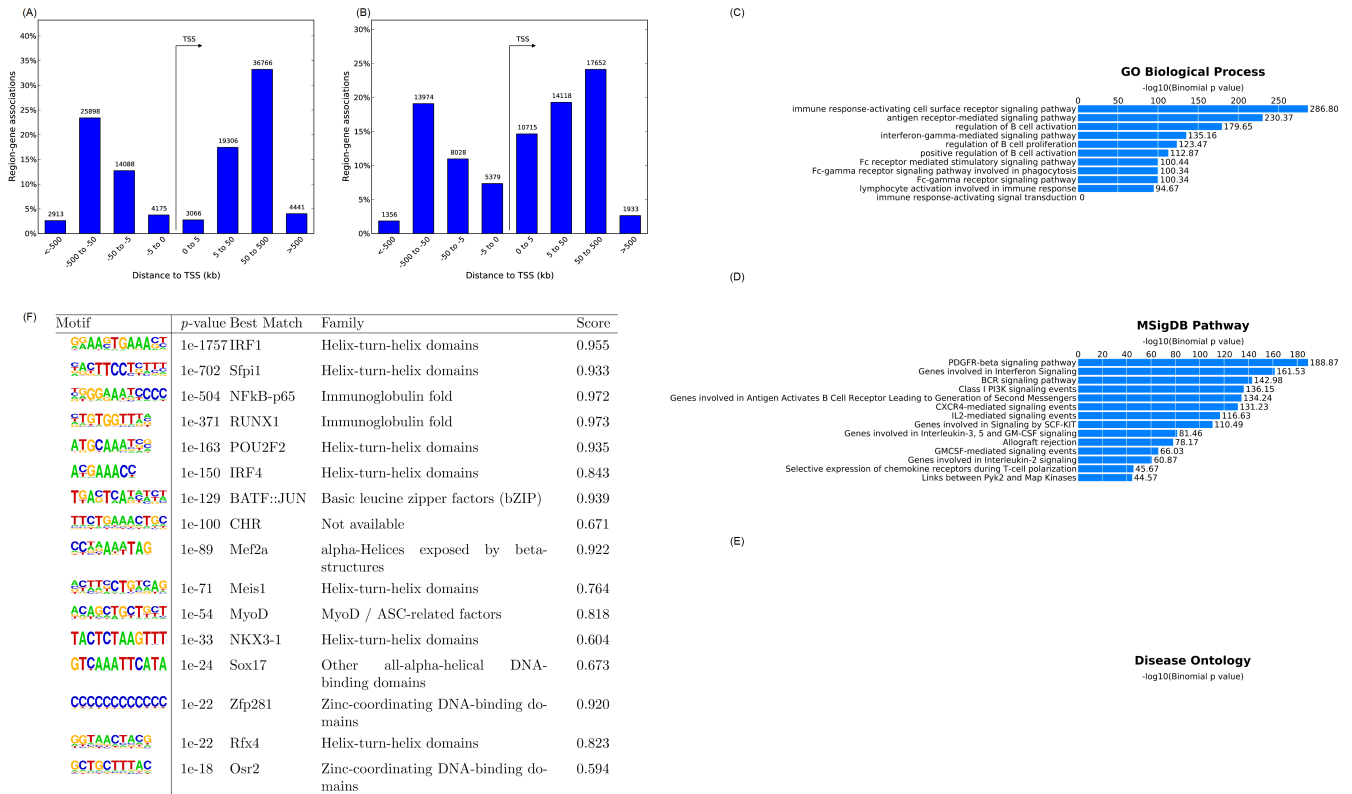


Figure S27: Functional and motif analysis of the Combined genome-wide predictions on cell line GM12878. A: Distance from the predicted A-Es to gene TSSs. B: Distance from the predicted A-Ps to gene TSSs. C,D,E: Top 20 enriched biological processes, pathways, and diseases, respectively, in the predicted cell-specific CRRs. F: Enriched *de novo* motifs in the predicted cell specific CRRs. Column 4: families of best-matched TFs. Column 5: best match scores.

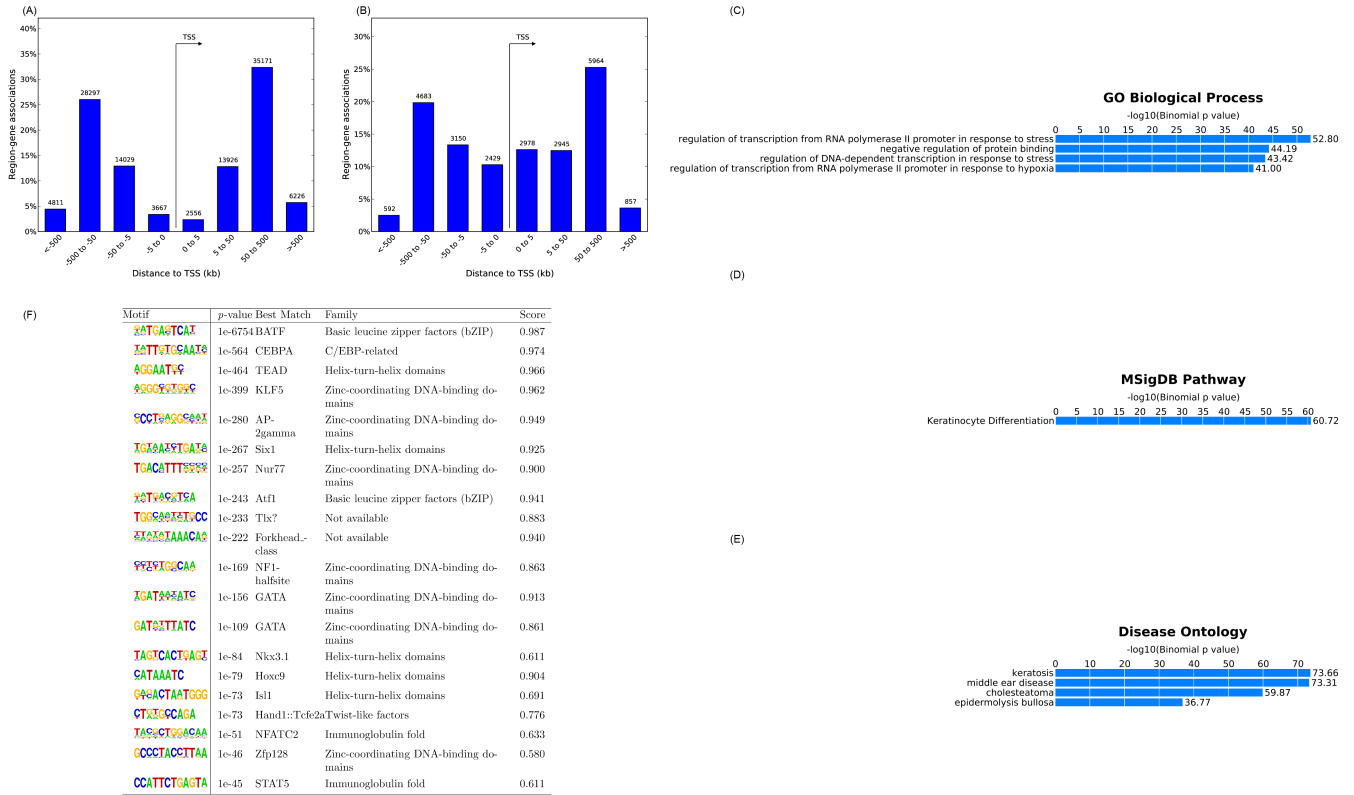
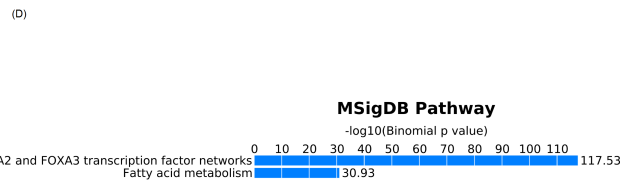
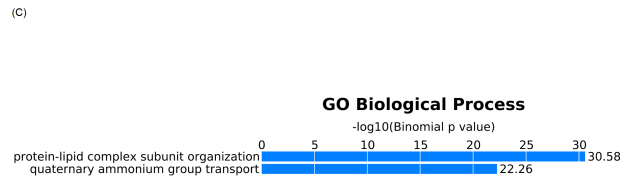
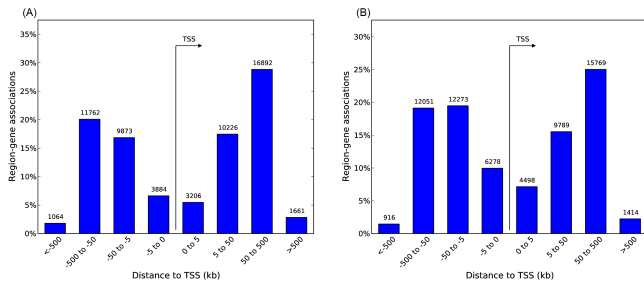


Figure S28: Functional and motif analysis of the Combined genome-wide predictions on cell line HeLaS3. A: Distance from the predicted A-Es to gene TSSs. B: Distance from the predicted A-Ps to gene TSSs. C,D,E: Top 20 enriched biological processes, pathways, and diseases, respectively, in the predicted cell-specific CRRs. F: Enriched *de novo* motifs in the predicted cell specific CRRs. Column 4: families of best-matched TFs. Column 5: best match scores.

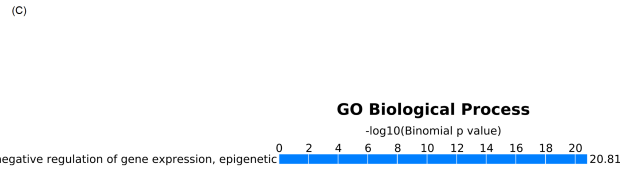
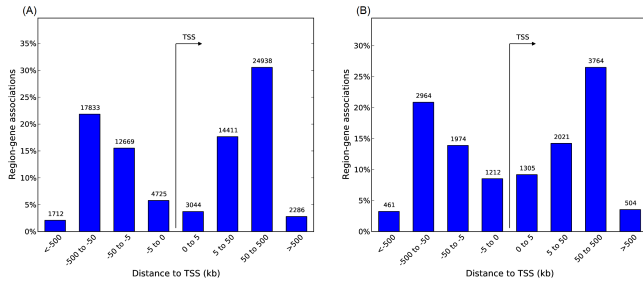


(F)

Motif	p-value	Best Match	Family	Score
GTCCAAAGTCA	1e-1086	HNF4A	Zinc-coordinating DNA-binding domains	0.968
CCCAAAGAS	1e-423	FoxEbox	Helix-turn-helix domains	0.904
TTAAATTAAC	1e-352	Hnf1	Helix-turn-helix domains	0.949
CTCCCTGGG	1e-101	Nr5a2	Zinc-coordinating DNA-binding domains	0.876
CCACCACTCA	1e-87	Six1	Helix-turn-helix domains	0.592
CATTCTGASCC	1e-74	MafA	Basic leucine zipper factors (bZIP)	0.632
TTGTGAAA	1e-68	CEBPA	C/EBP-related	0.901
AGCTGAG	1e-63	Nuclear Receptor class	Not available	0.786
ATACTCCCTTT	1e-61	Pou6f1	Helix-turn-helix domains	0.576
CCCGAGGGG	1e-60	KLF5	Zinc-coordinating DNA-binding domains	0.875
TSACTCTAG	1e-56	T	Basic helix-loop-helix factors (bHLH)	0.653
AGCCCAAGGAG	1e-49	Egr2	Zinc-coordinating DNA-binding domains	0.691
CAGGAAGCT	1e-48	EWS-ERGFusion	Helix-turn-helix domains	0.744
CCCTCCRC	1e-48	Tlx?	Not available	0.658
CCCGGCG	1e-47	Tcfap2e	Basic domains	0.715
CCCAATCC	1e-43	NFKB1	Immunoglobulin fold	0.733
GTCTAGCAATC	1e-42	Rfx3	Helix-turn-helix domains	0.670
CTAGGGAAGGA	1e-42	at_AC_aceptor	Not available	0.575
CTTGAAAAT	1e-41	NFATC2	Immunoglobulin fold	0.892
CGAAGCTGAAAC	1e-40	DCE.S.I	Not available	0.637



Figure S29: Functional and motif analysis of the Combined genome-wide predictions on cell line HepG2. A: Distance from the predicted A-Es to gene TSSs. B: Distance from the predicted A-Ps to gene TSSs. C,D,E: Top 20 enriched biological processes, pathways, and diseases, respectively, in the predicted cell-specific CRRs. F: Enriched *de novo* motifs in the predicted cell specific CRRs. Column 4: families of best-matched TFs. Column 5: best match scores.



Motif	p-value Best Match	Family	Score
AGATAAGGG	1e-2706 Gata2	Zinc-coordinating DNA-binding domains	0.980
TGCTGAGTCALIS	1e-630 Bach2	NF-E2-like factors	0.974
AAGAGGAAGT	1e-238 Sfp1	Helix-turn-helix domains	0.921
GGGGGGVXXXX	1e-227 KLF5	Zinc-coordinating DNA-binding domains	0.921
GCACCTCAGATIS	1e-202 CREB	CREB-like factors	0.600
TTCFAGGAAE	1e-176 STAT5	Immunoglobulin fold	0.948
TAGTACATCAA	1e-175 Six1	Helix-turn-helix domains	0.581
TAGGTAATCTC	1e-173 Spz1	Not available	0.667
TGTAAACTGTCA	1e-170 Myb	Helix-turn-helix domains	0.763
CCACCGTCCCC	1e-166 Zfp161	Zinc-coordinating DNA-binding domains	0.602
GAGTCCAGACA	1e-163 Tbox:Smad	Not available	0.805
GGCCGAGCTCA	1e-140 RXR	Zinc-coordinating DNA-binding domains	0.711
GTACCAGGTT	1e-133 Nkx3-1	Helix-turn-helix domains	0.546
GCAGACAGAAAG	1e-130 DCE.S.I	Not available	0.613
TTTTAGCCATA	1e-128 Zfp187	Zinc-coordinating DNA-binding domains	0.593
ATZACCATCCTA	1e-126 Pou2E3	Helix-turn-helix domains	0.639
GACCCGAAACAG	1e-121 DCE.S.I	Not available	0.611
CATCTTCCCTCC	1e-116 E2F2	Helix-turn-helix domains	0.632
GGTCTACAGCTA	1e-111 DCE.S.II	Not available	0.614
CCAGAAATCACC	1e-109 Hdx	Helix-turn-helix domains	0.749

(D)

MSigDB Pathway
-log10(Binomial p value)

(E)

Disease Ontology
-log10(Binomial p value)

Figure S30: Functional and motif analysis of the Combined genome-wide predictions on cell line K562. A: Distance from the predicted A-Es to gene TSSs. B: Distance from the predicted A-Ps to gene TSSs. C,D,E: Top 20 enriched biological processes, pathways, and diseases, respectively, in the predicted cell-specific CRRs. F: Enriched *de novo* motifs in the predicted cell specific CRRs. Column 4: families of best-matched TFs. Column 5: best match scores.

References

- [1] B. Arnett, P. Soisson, B.S. Ducatman, and P. Zhang. Expression of CAAT enhancer binding protein beta (C/EBP beta) in cervix and endometrium. *Molecular Cancer*, 2:21, 2003.
- [2] M. Beger, K. Butz, C. Denk, T. Williams, H.C. Hurst, and F. Hoppe-Seyler. Expression pattern of AP-2 transcription factors in cervical cancer cells and analysis of their influence on human papillomavirus oncogene transcription. *Journal of Molecular Medicine*, 79(5-6):314–320, 2001.
- [3] R.H. Costa, V.V. Kalinichenko, A.X. Holterman, and X. Wang. Transcription factors in liver development, differentiation, and regeneration. *Hepatology*, 38(6):1331–1347, 2003.
- [4] A. Dev, S. Iyer, B. Razani, and G. Cheng. NF- κ B and innate immunity. *Current Topics in Microbiology and Immunology*, 349:115–143, 2011.
- [5] J.D. Fleming, G. Pavesi, P. Benatti, C. Imbriano, R. Mantovani, and K. Struhl. NF-Y coassociates with FOS at promoters, enhancers, repetitive elements, and inactive chromatin regions, and is stereopositioned with growth-controlling transcription factors. *Genome Research*, 23(8):1195–1209, 2013.
- [6] D. Kleftogiannis, P. Kalnis, and V.B. Bajic. DEEP: A general computational framework for predicting enhancers. *Nucleic Acids Research*, 43(1):e6, 2015.
- [7] A.K. Linnemann, H. O’Geen, S. Keles, P.J. Farnham, and E.H. Bresnick. Genetic framework for GATA factor function in vascular biology. *Proceedings of the National Academy of Sciences*, 108(33):13641–13646, 2011.
- [8] R. Lopez, E. Garrido, G. Vazquez, P. Pina, C. Perez, I. Alvarado, and M. Salcedo. A subgroup of HOX Abd-B gene is differentially expressed in cervical cancer. *International Journal Gynecological Cancer*, 16(3):1289–1296, 2006.
- [9] A.L. Malt, J. Cagliero, K. Legent, J. Silber, A. Zider, and D. Flagiello. Alteration of TEAD1 expression levels confers apoptotic resistance through the transcriptional up-regulation of Livin. *PLoS One*, 7(9):e45498, 2012.
- [10] E.V. Mityushova, N.D. Aksenov, and I.I. Marakhova. STAT5 in regulation of chronic leukemia K562 cell proliferation: Inhibitory effect of WHI-P131. *Cell and Tissue Biology*, 4(1):63–69, 2010.
- [11] T. Okuda, M. Nishimura, M. Nakao, and Y. Fujita. RUNX1/AML1: A central player in hematopoiesis. *International Journal of Hematology*, 74(3):252–257, 2001.
- [12] G.V. Samant, M.O. Schupp, M. Francois, S. Moleri, R.K. Kothinti, C.Z. Chun, I. Sinha, S. Sellars, N. Leigh, K. Pramanik, M.A. Horswill, I. Remadevi, K. Li, G.A. Wilkinson, N.M. Tabatabai, M. Beltrame, P. Koopman, and R. Ramchandran. Sox factors transcriptionally regulate ROBO4 gene expression in developing vasculature in zebrafish. *The Journal of Biological Chemistry*, 286:30740–30747, 2011.
- [13] H. Schrem, J. Klempnauer, and J. Borlak. Liver-enriched transcription factors in liver function and development. Part II: The C/EBPs and D site-binding protein in cell cycle control, carcinogenesis, circadian gene regulation, liver regeneration, apoptosis, and liver-specific gene regulation. *Pharmacological Reviews*, 56(2):291–330, 2004.
- [14] C.C. Thornton, F. Al-Rashed, D. Calay, G.M. Birdsey, A. Bauer, H. Mylroie, B.J. Morley, A.M. Randi, D.O. Haskard, J.J. Boyle, and J.C. Mason. Methotrexate-mediated activation of an AMPK-CREB-dependent pathway: A novel mechanism for vascular protection in chronic systemic inflammation. *Annals of the Rheumatic Diseases*, 75(2):439–448, 2015.
- [15] P. Wang, J. Xu, and C. Zhang. CREB, a possible upstream regulator of Bcl-2 in trichosanthin-induced HeLa cell apoptosis. *Molecular Biology Reports*, 37(4):1891–1896, 2010.
- [16] Z. Wang, E.P. Bishop, and P.A. Burke. Expression profile analysis of the inflammatory response regulated by hepatocyte nuclear factor 4 α . *BMC Genomics*, 12:128, 2011.

- [17] H. Zhang, C. Liu, Z. Zha, B. Zhao, J. Yao, S. Zhao, Y. Xiong, Q. Lei, and K. Guan. TEAD transcription factors mediate the function of TAZ in cell growth and epithelial-mesenchymal transition. *The Journal of Biological Chemistry*, 284(20):13355–13362, 2009.
- [18] J. Zhu, D.M. Giannola, Y. Zhang, A.J. Rivera, and S.G. Emerson. NF-Y cooperates with USF1/2 to induce the hematopoietic expression of HOXB4. *Blood*, 102(7):2420–2427, 2003.